AD-A097 139 STANFORD UNIV CA INST FOR PLASMA RESEARCH F/6 3/2
MICROWAVE RADIO EMISSION FROM LOOP STRUCTURES IN THE SOLAR CHRO--ETC(U)
OCT 80 J F VESECKY N66001-80-C-0288
UNCLASSIFIED SU-IPR-823 NL

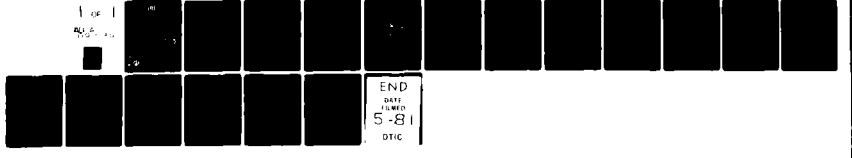

END
DATE FILMED
5-81
DTIC

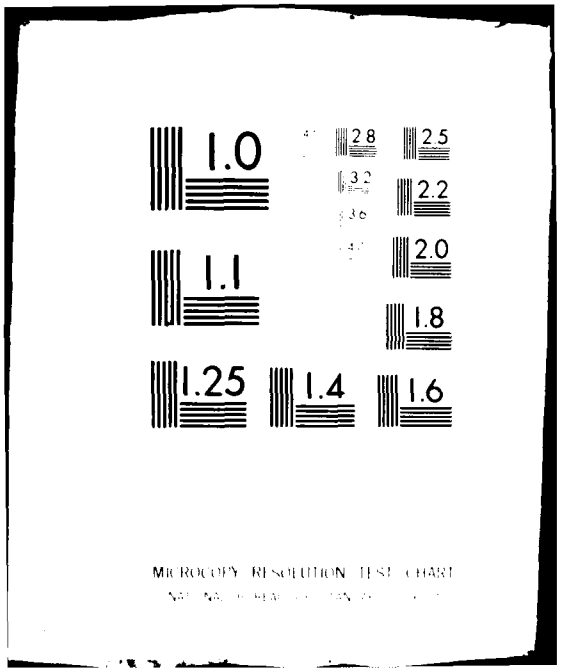
1.0
2.8
2.5
3.2
2.2
3.6
2.0
1.1
1.8
1.25
1.4
1.6
MICROCOPY RESOLUTION TEST CHART

LEVEL II

12

MICROWAVE RADIO EMISSION FROM LOOP STRUCTURES IN THE SOLAR CHROMOSOPHERE AND CORONA

by

John F. Vesecky

Office of Naval Research
Contract NOSC N66001-80-C-0288

SUIPR Report No. 823

October 1980

INSTITUTE FOR PLASMA RESEARCH
STANFORD UNIVERSITY, STANFORD, CALIFORNIA

MICROWAVE RADIO EMISSION FROM LOOP STRUCTURES IN THE SOLAR CHROMOSPHERE AND CORONA

by

John F. Vesecky*

Office of Naval Research
Contract NOSC/N66001-80-C-0288

SUIPR Report No. 823
October 1980

Institute for Plasma Research
Stanford University
Stanford, California

*Also Center for Radar Astronomy

ABSTRACT

Our overall objective in this research is to revisit the slowly varying or S component of solar microwave emission having in hand a much more detailed knowledge of active region structure than was available when the S component was studied extensively in the 1950's and 60's. In particular we want to consider the radio emission from the active region loop structures so evident in Skylab X-ray and UV images. In this initial report we investigate the distribution of microwave optical depth ($\tau_\perp$), brightness temperature (T_b) and emission per unit length (E) along model loops. In view of the large loop size (10^{10} cm total length) and short observation wavelengths, we have neglected gyroresonance absorption and considered only free-free absorption in computing optical depths. For loops of the same length observed at the same frequency, a low area factor (Γ = cross sectional area at loop apex/cross sectional area at loop base) loop exhibits an optical depth ($\tau_\perp$) which falls more rapidly with distance up the loop than does a high Γ loop. The perpendicular optical depth, $\tau_\perp$, is computed along a ray path perpendicular to the loop axis, i.e. $\tau_\perp$ corresponds to a limb observation of the loop. Brightness temperature $T_b^\perp$ also fall more rapidly with distance up the loop for a low Γ loop. Regarding the spatial distribution of microwave emission we find that for a Γ = 2 loop a significant, but not dominant, portion of the emission comes from the coronal portion of the loop. However, for a Γ = 50 loop the dominant microwave emission comes from the coronal portion of the loop. Thus for high Γ loops the relatively diffuse, but very hot plasma, in the large coronal volume of the loop emits more microwave energy than the much more dense, but cooler plasma, in the lower (chromospheric and transition region) portion of the loop. Future plans include calculations for a more varied selection of loop model parameters and observational geometries as well as comparisons with observations made at NOSC's La Posta solar microwave observatory.

I INTRODUCTION

Microwave radio emission from the Sun as a whole can be conveniently divided into three classes: The quiet Sun emission from the solar atmosphere in the absence of solar activity, a slowly varying or "S" component which rises and falls with changes in the number of active regions on the disc and hence with sunspot number, and short lived microwave bursts which last on the order of minutes and are often associated with flares. We are concerned here with the origin of the S component. This component received considerable study in the 1950's and 60's. Our objective here is to revisit the S component having in hand a much more detailed knowledge of active region structure than was previously available. In particular we want to consider the effects of active region loops--the dense, high temperature structures so prominent in UV and X-ray images of the chromosphere and corona (Fig. 1).

As a beginning, we have looked at the spatial distribution of microwave optical depth (τ), microwave brightness temperature (T_b) and microwave emission per unit length (E) along model loops. For our model loops (see Vesecky, Antiochos and Underwood, 1979) we also answer the question: What percent of the total microwave emission arises from the lower 10%, 20%, etc. of the loop. Interestingly, we find that for loops with large values of the area ratio (Γ = cross sectional area at loop top divided by cross sectional area at loop base) the optically thin, but hot ($T \sim 10^6$ K), coronal portion of the loop emits more microwave energy than the optically thick, but cool ($T \sim 5 \times 10^4$ K), chromospheric portion of the loop.

In these calculations we have not considered gyroresonance absorption. Kunder, Schmahle and Gerassimenko (1980) argue that gyroresonance is the dominant mechanism for absorption in some cases since in their observations of McMath 12379 they find that the radio brightness temperature and plasma temperatures (deduced from EUV and X-ray observations) are comparable and free-free absorption is not sufficiently strong to achieve the required unity optical depth. For the large loop size considered here (10^{10} cm total length) the magnetic field near the top of the loop is presumably small ($\lesssim 100$ gauss) and hence the gyrofrequency much smaller than the primary observing frequencies (15 and 35 GHz). So we have neglected gyroresonance absorption. Calculation for smaller loops and lower observing frequencies should include gyroresonance absorption. Future plans include calculations for a more varied selection of loop model parameters and observational geometries as well as comparisons with observations made at NOSC's La Posta solar microwave observatory.

II MICROWAVE τ, T_b AND EMISSION DISTRIBUTION FOR MODEL LOOPS

Loop Models: To estimate τ, T_b and the emission distribution for an active region loop one needs to know the physical conditions inside the loop (temperature T and electron number density n). We use the loop model of Vesecky, Antiochos and Underwood (1979), hereafter VAU, which numerically

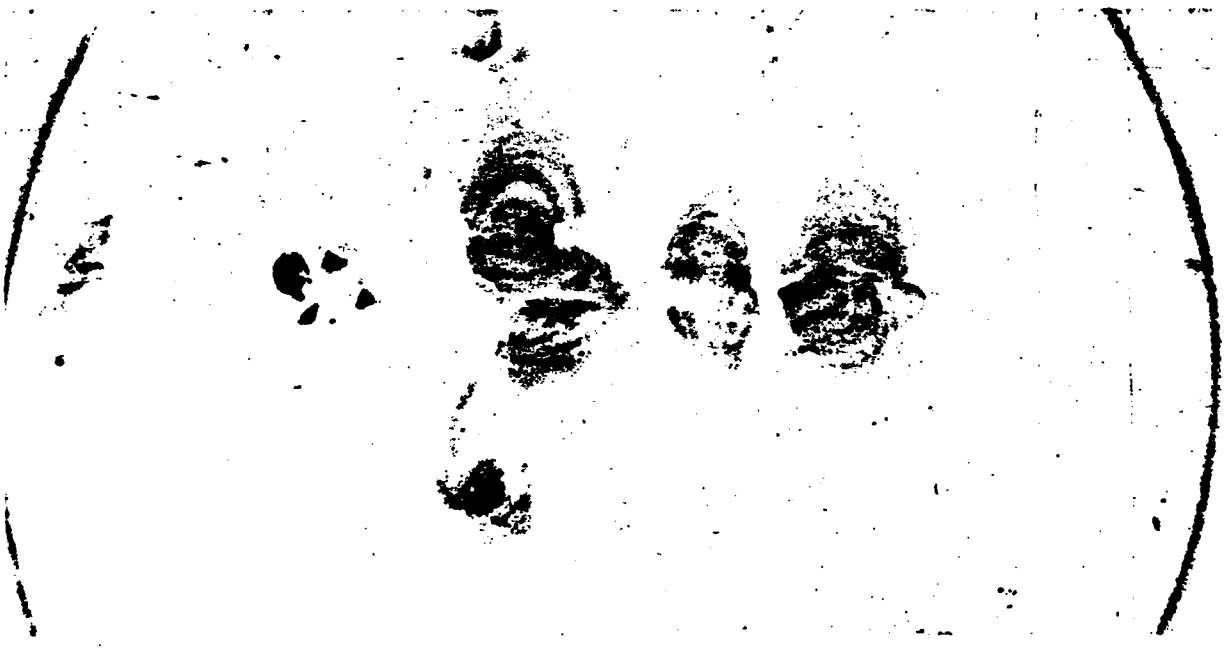

Fig. 1. Skylab UV (Fe XV) image of the solar disc at midlatitudes showing loop structures at temperatures of around 2.5 X 10^6 K. The image is a negative print with blacker features being in fact brighter on the Sun. It is clear that the structure above an active region consists of an ensemble of loops having various lengths, temperatures, densities, etc. The Naval Research Laboratory S-055 ultraviolet spectrometer on Skylab obtained the image which was subsequently published by Eddy (1979).

integrates the momentum and energy balance equations up the loop in a sequence of trials until boundary conditions at the loop base and apex are satisfied. The boundary conditions are T=30,000K at the base of the loop, presumed to be in the upper chromosphere, and dT/ds =0 at the base and apex of the loop, s being the coordinate along the loop (see Fig. 2). The vanishing of the temperature gradient at the loop apex follows from the assumption that the loop is symmetric about the apex.

The geometric form of the loop is assumed to be that of a line dipole magnetic field. For a line dipole, magnetic field lines are circles passing through the dipole origin as shown in Fig. 2. Such a magnetic flux tube, which confines the plasma constituting the loop, can be defined by noting the length ℓ and area of the flux tube (perpendicular to the magnetic field line defining the axis of the loop) at both the base A_b and the apex A_a. The area factor Γ relates these two areas $\Gamma = A_a/A_b$. Here we take A_b to be the size of a typical flux concentration observed by Tarbell and Title (1977) namely an area of $\sim$ 1000 km diameter with a magnetic flux density of $\sim$ 1000 gauss ; hence $A_b \sim 8 \times 10^{15}$ cm ^{2}. Solar UV and X-ray observations such as Pye et al. (1978) suggest that $A_a \sim 10^{17}$ to 10^{18} cm ^{2}. For consideration here we take $A_a \sim 4 \times 10^{17}$ cm^2 yielding $\Gamma = 50$ and consider a large loop of length $\ell = 10^{10}$ cm as suggested by the aforementioned UV and X-ray observations. We also examine a $\Gamma = 2$ loop for comparison purposes. For a line dipole magnetic field ℓ and Γ determine h and d in Fig. 2 via the equations $\Gamma = h/d$ and $\ell = 2h \cos^{-1}(\Gamma^{-1/2})$.

We note here that UV and X-ray observations alone would not suggest such a large value of Γ. In fact most UV or X-ray images of the Sun suggest that Γ is on the order of 1 to 3 (see VAU). Based on Tarbell & Title's (1977) observations of photospheric magnetic fields, we argue that Γ is in fact much larger and that the portion of a loop structure which has a small area is simply not seen in most UV and X-ray images because it is both small in emitting volume and relatively cool.

The consequences of a large value of Γ are illustrated by VAU. In general relatively larger portions of the mass of a loop structure are located in the coronal part of the loop where temperatures are high. This increases the differential emission measure (with respect to temperature) of the upper portion of a loop relative to a low Γ case. Hence one would expect relatively more optically thin microwave emission (which arises in the less dense, upper portion of a loop) from high Γ loops.

Microwave Absorption Coefficient: If one considers a plasma with electrons moving in response to an applied electromagnetic wave, the equation of motion of an electron contains a term proportional to electron velocity and to the rate of "collisions" between electrons and ions, ν_c. This term gives rise to absorption as the wave propagates through the medium. This absorption is characterized by an absorption coefficient K such that the wave electric field varies as

$$\vec{E}(r,t) = \vec{E}_o e^{-(Kr/2)} \cos(kr - \omega t)$$

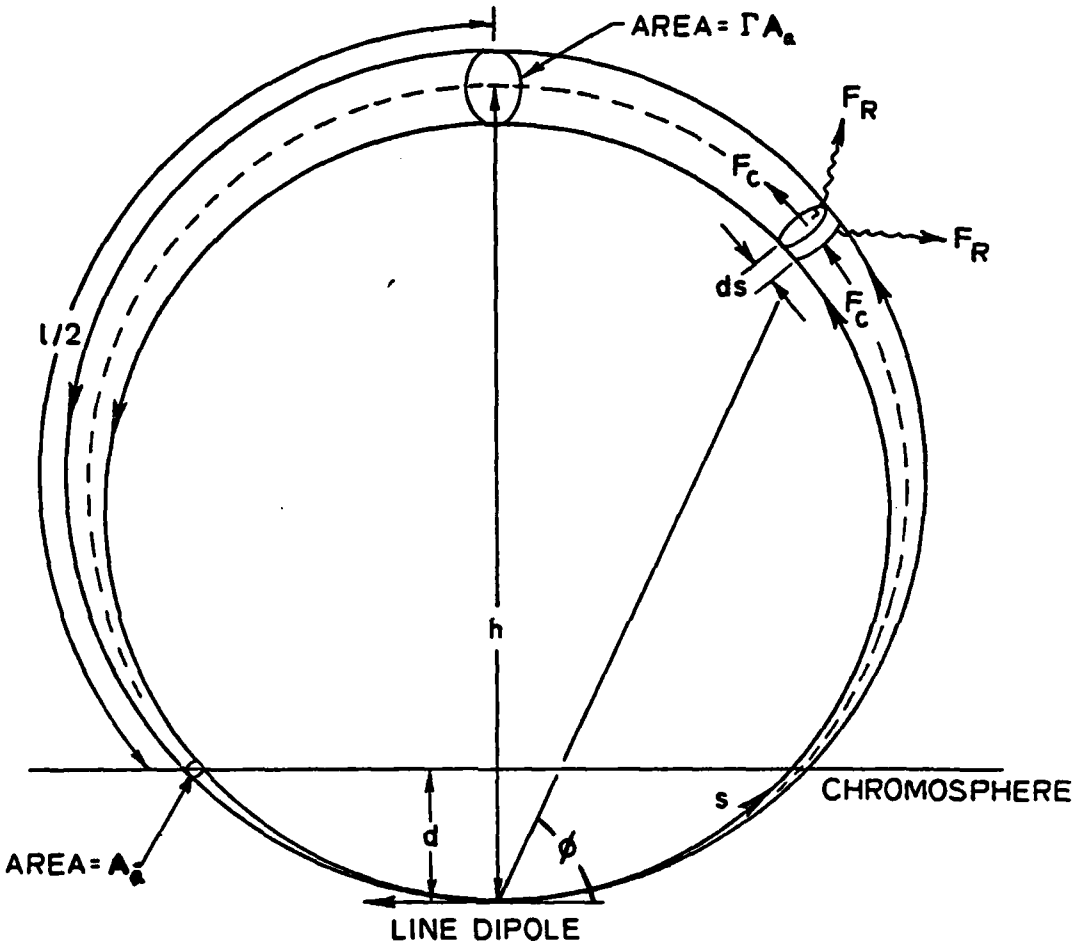

Fig. 2. Coronal loop geometry for line dipole magnetic field. The origin of the line dipole is located at a depth d below the loop base (taken to be at the 30,000 K level in the upper chromosphere). The area factor Γ is defined as the ratio of the loop cross-sectional area at the apex to that at the base. The coordinate s is along the magnetic field line. A volume element dV, having dimension ds along and radius $\rho(s)$ perpendicular to the magnetic field is shown with radiative (F_R) and convective fluxes (F_C) indicated schematically.

For wave frequencies $\omega >> \nu_c$ or ω_p (the electron-ion collision frequency, and electron plasma frequency respectively) Harwit (1973) quotes for a hydrogen plasma

$$K(\nu) = \frac{8}{3\sqrt{2\pi}} \frac{e^6 n^2}{c(mkT)^{3/2} \nu_c^2} \ln \left[\frac{1.32 (kT)^{3/2}}{2\pi e^2 m^{1/2} \nu_c} \right], \quad (1)$$

where n is the electron number density, m the electron mass and cgs units are used. This expression is sufficient for our purposes.

Optical Depth Calculation: Optical depth is given by

$$\tau(\nu, T, n) = \int_{path} K(\nu, T, n)\, dx \quad (2)$$

where the path lies through the emitting region. For the cases at hand $\omega >> \omega_p$ and thus sufficiently little refraction occurs that we can take a straight line ray path through the loop. Initially we will consider ray paths passing through the loop along lines perpendicular to the plane of Fig. 2. Assuming the loop to have a circular cross section, the average distance through the loop is $(4/\pi)$ times the loop radius $\rho(s)$, where ρ is measured perpendicular to the loop axis. Since the loop model assumes variation only along the loop axis, i.e. along s in Fig. 2., the average optical depth $\tau_\perp$ is:

$$\tau_\perp(s,\nu) = (4/\pi)\rho(s)\, K\left[\nu, n(s), T(s)\right]. \quad (3)$$

Geometrical considerations show that the cross sectional area of the loop $A(s) = A_a \sin^2 \phi$ where ϕ is the polar angle shown in Fig. 2. Since $A(s) = \pi\rho^2(s)$, further analytic geometry yields: $\rho(s) = (A_a/\pi)^{1/2} \sin(s/h)$ and the average perpendicular optical depth becomes

$$\tau_\perp(s) = (16\, A_a/\pi)^{1/2} \sin(s/h)\, K(\nu, n, T) \quad (4)$$

Brightness Temperature Calculation: Knowing the optical depth and temperature along the loop $\tau_\perp(s)$ and T(s) it is a simple matter to calculate the brightness temperature $T_b(s)$ for ray paths passing through the loop while perpendicular to the plane of the loop, i.e. perpendicular to the plane of Fig.2. Following Kraus (1966) we find that

$$T_b = T_s\, e^{-\tau_\perp} + T\,(1 - e^{-\tau_\perp}) \quad (5)$$

Where T_s is the brightness temperature of the background against which the model loop is viewed. Since our case corresponds to a loop on the solar limb, we will take $T_s = 0$.

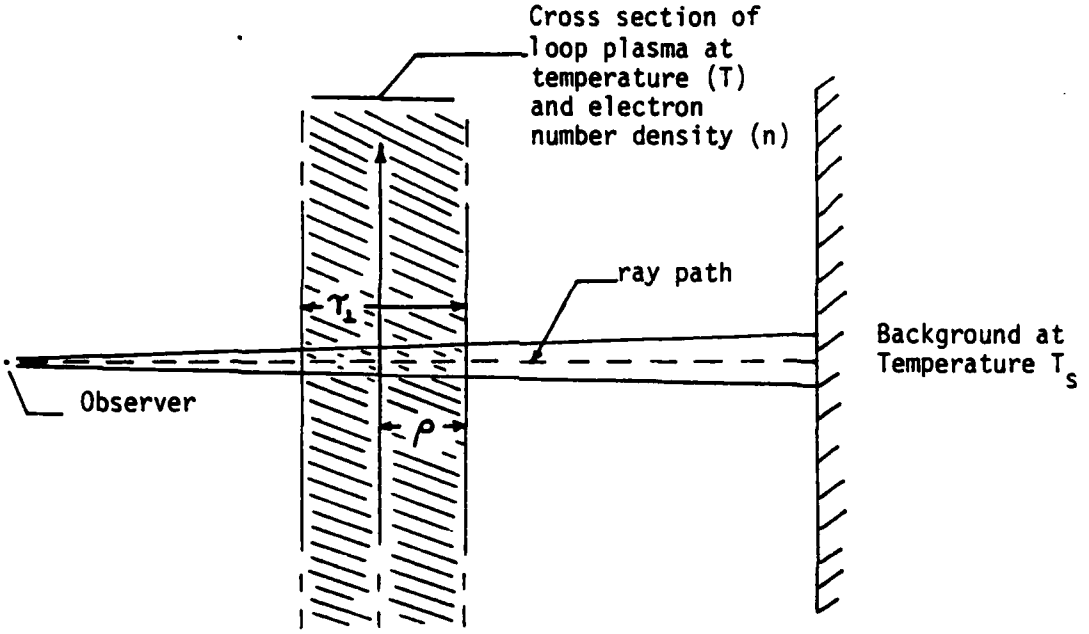

Fig. 3. Schematic diagram of brightness temperature calculation.

Emission from an Elementary Volume of Loop: *Once T_b is known* we can find the microwave flux arising from an elementary volume of Loop dV (Fig. 2) when viewed along a ray path perpendicular to the plane of the loop. For an observer at some fixed distance from the loop, the flux dF from dV is simply proportional to the brightness temperature times the area of dV perpendicular to the ray path (Kraus, 1966), i.e.

$$dF \propto T_b \, \rho ds. \tag{6}$$

Emission Distribution along the Loop: To characterize the distribution of microwave emission along the model loop we need to answer the question: What fraction of the total microwave emission arises from a given fraction of the loop, e.g. the bottom 10%, 20%, etc. Here we refer to the total emission observed along ray paths perpendicular to the plane of the loop, not the total emission of the loop in all directions. To answer our question we calculate the quantity Φ given by

$$\Phi(f) = F(f)/F_1 = F_1^{-1} \int_{s_b}^{s_f} dF = F_1^{-1} \int_{s_b}^{s_f} T_b \, \rho ds \tag{7}$$

where $s_f = [(f\ \ell/2) + s_b]$, $s = s_b$ at the base of loop, $s_b = h \sin^{-1} \sqrt{d/h}$ and $F_1 = F(f=1)$. The function $\Phi(f)$ characterizes the relative importance of the coronal and chromospheric portions of the loop. For example, if $\Phi(f) = f$ then all portions of the loop are equally important. If $\Phi(f) > f$ near the top of the loop ($f \sim 1$), then the coronal portion of the loop is most important when interpreting microwave radio observations. Conversely if $\Phi(f) < f$ for $f \sim 1$, the chromospheric and transition region portions dominate.

III RESULTS

By way of results we will show $\tau_\perp(s)$, $T_b(s)$ and $\Phi(f)$ for four different cases. The parameters for these cases are given in Table I. Basically we examine 3 cases of varying observational wavelength with Γ=50 and one case where Γ=2 for comparison.

Optical Depth: In Fig. 4 we plot the perpendicular optical depth ($\tau_\perp$) as a function of distance up the loop from the base ($s - s_b$). Both ordinate and abscissa scales are logarithmic in order to show the large range of variation. Although we show results close to the loop base (dashed lines) to assure the reader that no unexpected variations occur, these results should not be taken as physically meaningful since near the loop base radiative transfer effects for large optical depths come into play. Gyroresonance absorption may also be important. Close to the loop base $\tau_\perp$ becomes asymptotically constant simply because the distance scale is so small that virtually no change in density, temperature or loop cross-sectional radius is taking place. Cases one through three represent the same model loop, but observing wavelengths of 1, 2 and 10 cm respectively. The level (distance from loop base) at which $\tau_\perp = 1$ rises as wavelength increases moving from 1.5 km above the base (λ_{obs}= 1 cm) to 28 km above the base (λ_{obs} = 10 cm). The point at which $\tau_\perp = 1$ corresponds to temperatures of 42,000; 64,000; and 170,000K for observing wavelengths of 1, 2 and 10 cm respectively. Comparing cases two and four we note that for a constant observing frequency the change in loop Γ from 50 to 2 makes relatively little difference near the base of the loop. Near the top of the loop the difference between the Γ= 50 and Γ= 2 loops, cases (1, 2 and 3) and case 4 respectively, becomes quite marked. For high Γ loops $\tau_\perp$ levels off in the upper portion of the loop while for the low Γ loop (case four) $\tau_\perp$ continues a power law decrease until near the apex of the loop. This behavior is due not only to the geometric difference between the high and low Γ loops, but also to the relatively higher density in the high Γ loops.

Brightness Temperature: The concept of brightness temperature in radio astronomy refers to the temperature of a fictitious black body filling the antenna beam which would produce the observed microwave energy flux (for further information see Kraus, 1966). The brightness temperature T_b, calculated

TABLE I

LOOP PARAMETERS

CASE	LENGTH (ℓ)	AREA FACTOR (Γ)	A_{base}	A_{apex}	n_{base}	n_{apex}	T_{base}	T_{apex}	λ_{obs}
(1)	10^{10}cm	50	8xk0^{15}cm^2	4x10^{17}cm^2	5.0x10^{10}cm^{-3}	7.3x10^{8}cm^{-3}	30x10^4 K	1.2x10^6 K	1 cm
(2)	10^{10}cm	50	8x10^{15}cm^2	4x10^{17}cm^2	5.0x10^{10}cm^{-3}	7.3x10^{8}cm^{-3}	30x10^4 K	1.2x10^6 K	2 cm
(3)	10^{10}cm	50	8x10^{15}cm^2	4x10^{17}cm^2	5.0x10^{10}cm^{-3}	7.3.x10^{8}cm^{-3}	30x10^4 K	1.2x10^6 K	10 cm
(4)	10^{10}cm	2	8x10^{15}cm^2	1.6x10^{16}cm^2	3.4x10^{10}cm^{-3}	4.3x10^{8}cm^{-3}	30x10^4 K	1.5x10^6 K	2cm

Notes

1. The energy input to all four model loops is 10^{-4} ergs cm^{-3} s^{-1} uniformly distributed throughout the loop.

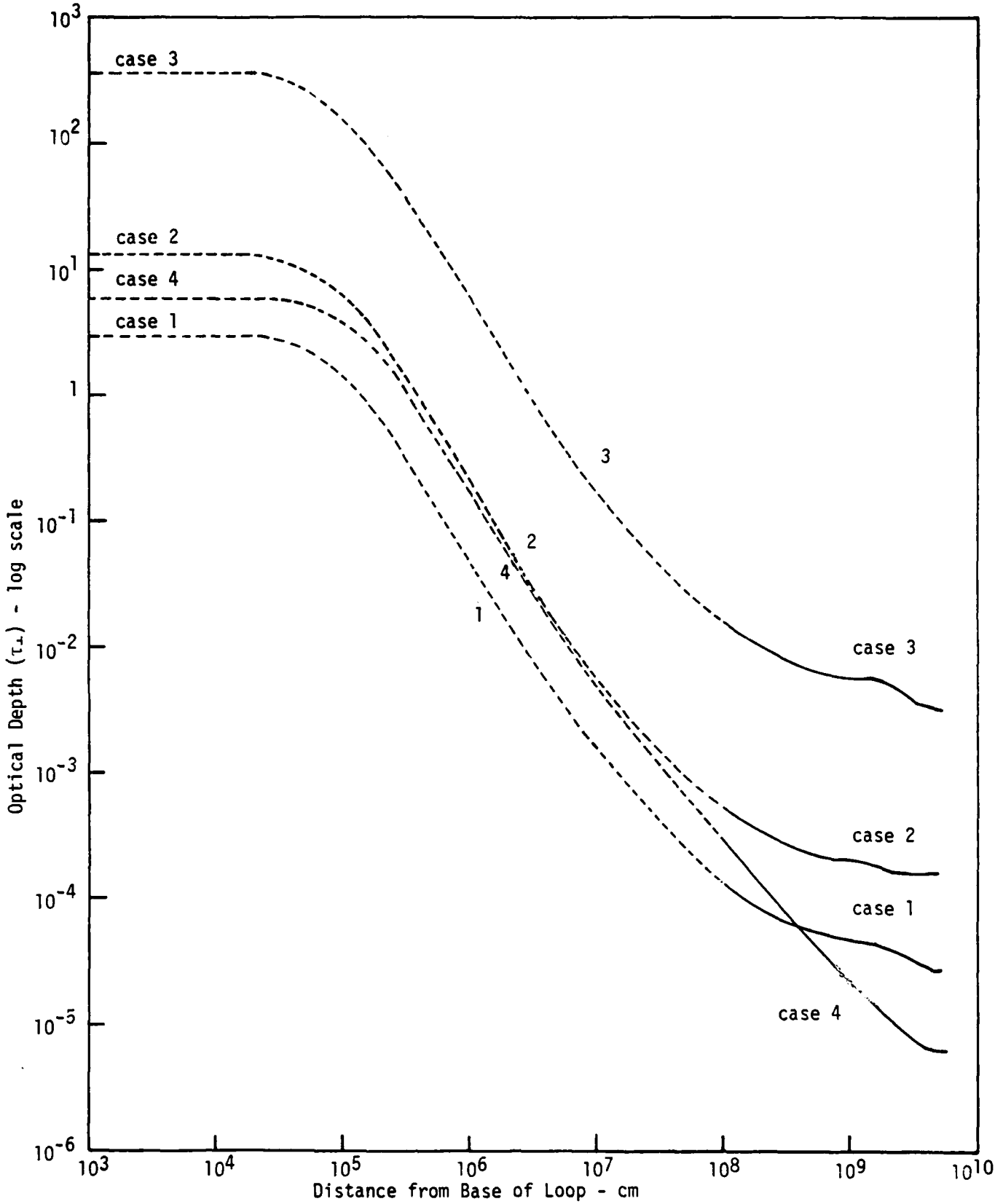

Fig. 4. Optical depth perpendicular to the plane of the loop ($\tau_\perp$) for various observing wavelengths and two loop geometries. $\tau_\perp$ is plotted as a function of distance upward from the base to the top of the loop. Cases 1, 2 and 3 are for a loop of length 10^{10} cm with area factor $\Gamma = 50$ at observational wavelengths of 1, 2 and 10 cm respectively. Case 4 is for a loop of the same length but with $\Gamma = 2$, observed at 2 cm wavelength. Values of optical depth for base distances less than 10^8 cm are probably not physically meaningful, but are shown as dashed lines to indicate the implications of the model in this region.

according to eq.(5), is shown in Fig. 5 as a function of distance upward from the base of the loop. In the calculation we have let T_s, the background temperature, go to zero. Referring to Fig. 4 we find that the peak value of T_b in Fig. 5 occurs slightly below the level where $\tau_\perp = 1$. Comparing cases 2 and 4 for $\Gamma = 50$ and 2 respectively but the same observational wavelength (2 cm) we find that T_b is lower for the low Γ loop especially near the apex where there is more than an order of magnitude difference. The lower T_b for case 4 is due to lower $\tau_\perp$ (see Fig. 4). In fact, near the apex, case 4 has a higher plasma temperature than case 2. As with $\tau_\perp$ in Fig. 4, T_b levels out in the upper portion of the loop.

Emission Distribution: Perhaps the most important question to be addressed here is whether the upper, coronal portion or the lower, chromospheric portion of a loop is most important in producing microwave emission. A correct interpretation of solar microwave observations depends on this question. In Fig. 6 we plot $\bar{\Phi}$ (f) from equation (7) for the four cases of Table I. A careful perusal of Fig. 6 shows that for the high Γ loop model the hot, but optically thin, coronal portion of the loop produces most of the microwave emission regardless of observational wavelengths. This effect is somewhat more pronounced at longer wavelengths, c.f. cases 1, 2 and 3. By contrast, the low Γ loop produces its microwave emission much lower down. Comparing cases 2 and 4 we find that for 2 cm observations the $\Gamma = 50$ loop produces 50% of its microwave emission in the top 40% of the loop whereas the $\Gamma = 2$ loop produces 50% of its microwave emission in the bottom 5% of the loop.

IV CONCLUSIONS & IMPLICATIONS

Fig. 6 sums up the conclusions of our calculations thus far. It shows quantitatively that for active region loop structures with large area factors ($\Gamma = 50$) the upper, coronal portion of the loop dominates the microwave emission. Conversely for $\Gamma = 2$ the lower portion of the loop dominates. However, even for the $\Gamma = 2$ case significant microwave emission does come from the coronal portion of the loop. To sum up, the hot, dense plasma confined in active region loops appears to radiate an important (and dominant in high Γ cases) portion of the microwave emission from the structure as a whole. This occurs in spite of the fact that these hot gases are optically thin ($\tau_\perp \lesssim 10^{-3}$) at microwave frequencies. The large volume and high temperature of the upper loop more than make up for the low value of τ

Since the chromosphere and corona above active regions is largely filled by loop structures, it is important to take these structures into account in the interpretation of microwave observations. At this point we have examined

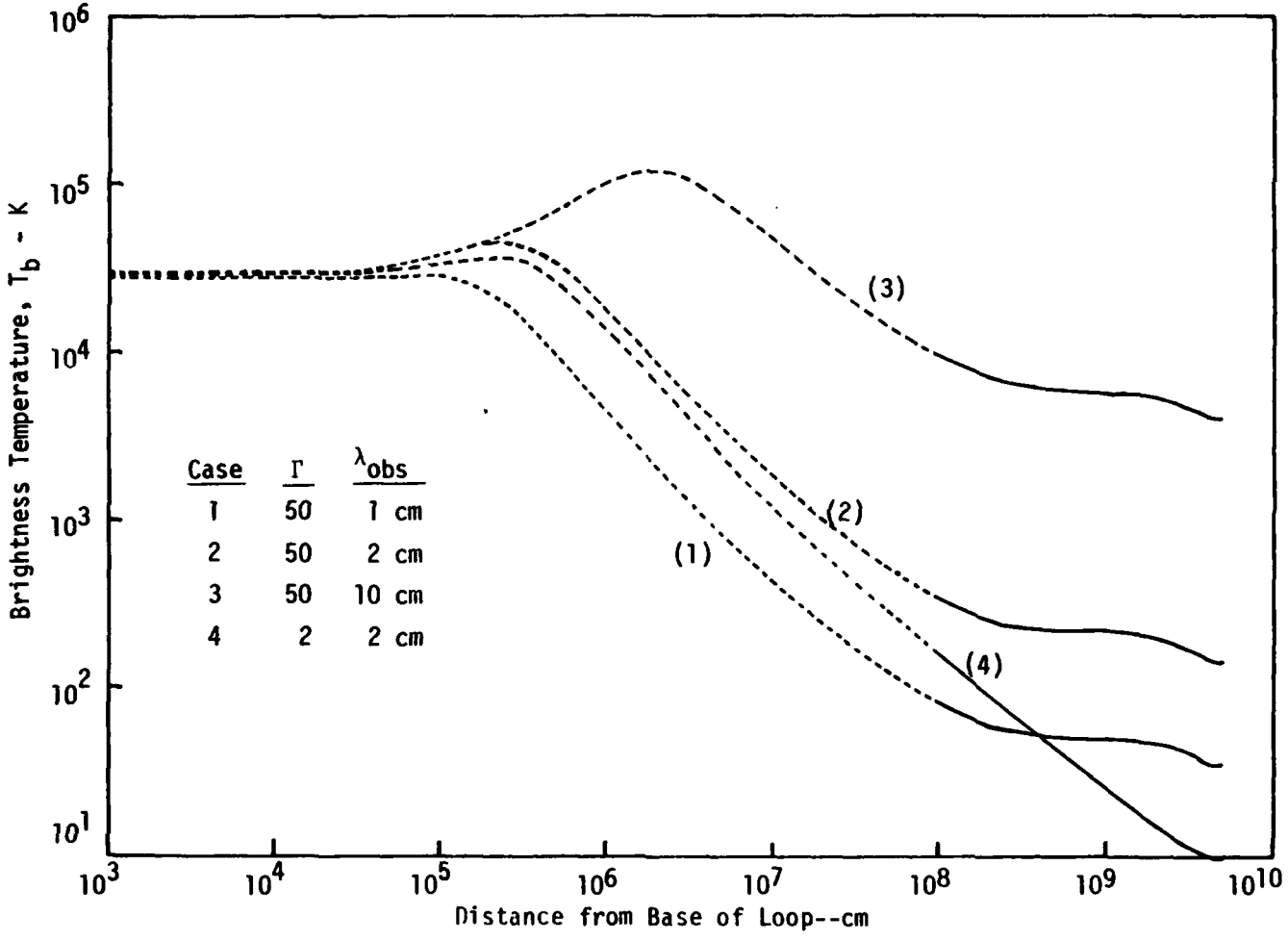

Fig. 5. Brightness temperature as a function of distance upward from loop base. All loops have a total length of 10^{10} cm. Further details on cases 1-4 are in Table I. Note that T_b for high Γ loop is nearly constant in the upper portion of the loop (~top 90%). Values of brightness temperature for base distances less than 10^8 cm are probably not physically meaningful, but are shown as dashed lines to indicate the implications of the model in this region.

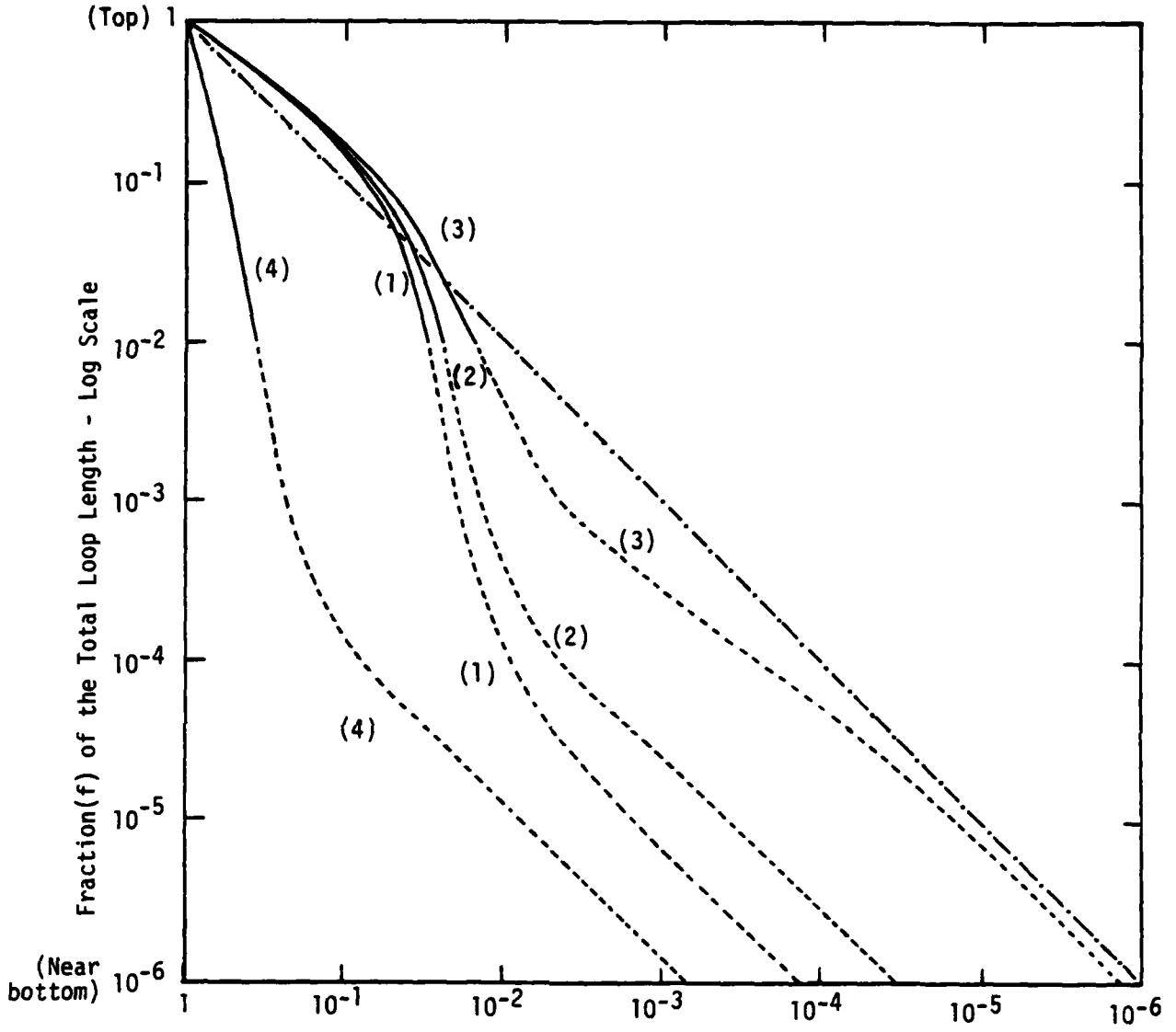

Fig. 6. Distribution of microwave emission for model loops. (This figure may be a little hard to understand at first, but you will find it worthwhile). For the four model loops summarized in Table I we show the fraction of total microwave emission, arising from the lower fraction f of the loop $\Phi(f)$. The dash-dot line corresponds to uniform emission along the length of the loop. For example, we see that for loops 1, 2 and 3 (where $\Gamma=50$) the top 90% of the loop ($f=10^{-1}$) provides about 93% of the emission, i.e. the hot coronal portion of the loop dominates the microwave emission. For loop 4 ($\Gamma=2$) the lower portion of the loop is dominant. Values of $\Phi(f)$ calculated for $f \lesssim 10^{-2}$ are probably not physically meaningful, but are shown as dashed lines to indicate the implications of the model in this region.

only two model loops for one observational geometry and three observing wavelengths. Active regions contain an ensemble of loops varying in size and physical characteristics. Nevertheless, it appears from our arguments here that these loops typically have high values of Γ. From Fig. 5 we would tentatively conclude that microwave observations of active regions should be interpreted in terms of the hot coronal portions of active region loops (a few tens of thousands of km above the chromosphere) rather than in terms of chromospheric and transition region plasmas in the active region.

ACKNOWLEDGMENT

The author would like to express his gratitude to Michal Plume, Kim Fisher and Martha Smith for help in preparing the manuscript and figures. This work was supported in part by ONR Contract NOSC N66001-80-C-0288.

REFERENCES

Eddy, J.A.: 1978, A New Sun: The Solar Results from Skylab, NASA SP-402, National Aeronautics & Space Administration, Washington, D.C.

Harwitt, M.: 1973, Astrophysical Concepts, Wiley: New York, p. 226.

Kundu, M.R., Schmahl, E.J., and Gerassimenko, M.: 1980, Astron. Astrophys., 82, 265-271.

Pye, J.P., Evans, K.D., Hutcheon, R.J., Gerassimenko, M., Davis, J.M., Krieger, A.S., and Vesecky, J.F.: 1978, Astron. Astrophys., 65, 123-138.

Tarbell, T.D., and Title, A.M.: 1977, Solar Phys., 52, 13-25.

Vesecky, J.F., Antiochos, S.K., and Underwood, J.H.: 1979, Ap. J., 233, 987-997.

UNCLASSIFIED

SECURITY CLASSIFICATION OF THIS PAGE (When Data Entered)

REPORT DOCUMENTATION PAGE	READ INSTRUCTIONS BEFORE COMPLETING FORM
1. REPORT NUMBER: SUIPR Report No. 823	2. GOVT ACCESSION NO.: AD-A097 139
	3. RECIPIENT'S CATALOG NUMBER
4. TITLE (and Subtitle): MICROWAVE RADIO EMISSION FROM LOOP STRUCTURES IN THE SOLAR CHROMOSPHERE AND CORONA	5. TYPE OF REPORT & PERIOD COVERED: Scientific, Technical
	6. PERFORMING ORG. REPORT NUMBER
7. AUTHOR(s): John F. Vesecky	8. CONTRACT OR GRANT NUMBER(s): ONR NOSC N66001-80-C-0288
9. PERFORMING ORGANIZATION NAME AND ADDRESS: Institute for Plasma Research, Stanford University, Stanford, California	10. PROGRAM ELEMENT, PROJECT, TASK AREA & WORK UNIT NUMBERS
11. CONTROLLING OFFICE NAME AND ADDRESS: Office of Naval Research, Durand 165, Stanford University	12. REPORT DATE: October 1980
	13. NUMBER OF PAGES: 14
14. MONITORING AGENCY NAME & ADDRESS (if different from Controlling Office)	15. SECURITY CLASS. (of this report): Unclassified
	15a. DECLASSIFICATION/DOWNGRADING SCHEDULE

16. DISTRIBUTION STATEMENT (of this Report)

This document has been approved for public release and sale; its distribution is unlimited.

17. DISTRIBUTION STATEMENT (of the abstract entered in Block 20, if different from Report)

18. SUPPLEMENTARY NOTES

19. KEY WORDS (Continue on reverse side if necessary and identify by block number)

Active Regions, Radio Emission, Loop Geometry

20. ABSTRACT (Continue on reverse side if necessary and identify by block number)

The overall objective in this research is to revisit the slowly varying or S component of solar microwave emission having in hand a much more detailed knowledge of active region structure than was available when the S component was studied extensively in the 1950s and 1960s. In particular we want to consider the radio emission from the active region loop structures so evident in Skylab X-ray and UV images..

DD FORM 1 JAN 73 1473 EDITION OF 1 NOV 65 IS OBSOLETE
S/N 0102 LF 014 6601

UNCLASSIFIED

SECURITY CLASSIFICATION OF THIS PAGE (When Data Entered)


DATE
ILMED
-8